

Supplementary Materials

A Dy(III) Fluorescent Single-Molecule Magnet Based on a Rhodamine 6G Ligand

Lin Miao ¹, Mei-Jiao Liu ¹, Man-Man Ding ², Yi-Quan Zhang ^{2,*} and Hui-Zhong Kou ^{1,*}

¹ Department of Chemistry, Tsinghua University, Beijing 100084, China; ml19@mails.tsinghua.edu.cn (L.M.); liumeijiao1024@126.com (M.-J.L.)

² Jiangsu Key Laboratory for NSLSCS, School of Physical Science and Technology, Nanjing Normal University, Nanjing 210023, China; 191002019@njnu.edu.cn (M.-M.D.)

* Correspondence: zhangyiquan@njnu.edu.cn (Y.-Q.Z.); kouhz@mail.tsinghua.edu.cn (H.-Z.K.)

1. Powder XRD of Complex 1

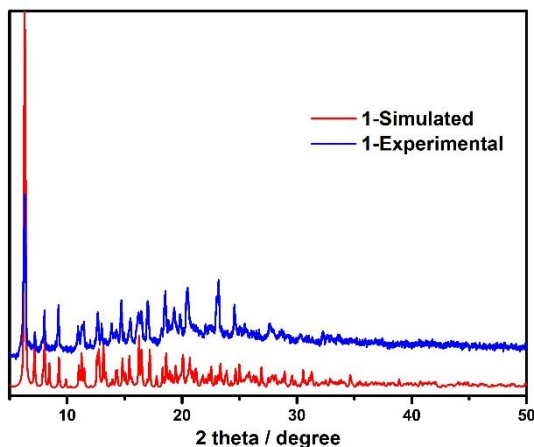


Figure S1. The powder XRD for Complex 1.

2. Magnetic Results

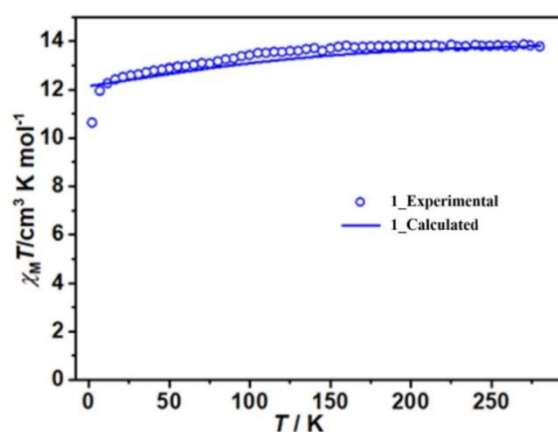


Figure S2. Variable-temperature magnetic susceptibilities for **1** under 2000 Oe applied field. The solid lines represent the calculated results, which was simulated by the program SINGLE_ANISO.

Citation: Miao, L.; Liu, M.-J.; Ding, M.-M.; Zhang, Y.-Q.; Kou, H.-Z. A Dy(III) Fluorescent Single-Molecule Magnet based on a Rhodamine 6G Ligand. *Inorganics* **2021**, *9*, 51. <https://doi.org/10.3390/inorganics9070051>

Academic Editor: Akseli Mansik-kämäki

Received: 31 May 2021

Accepted: 26 June 2021

Published: 29 June 2021

Publisher's Note: MDPI stays neutral with regard to jurisdictional claims in published maps and institutional affiliations.



Copyright: © 2021 by the authors. Licensee MDPI, Basel, Switzerland. This article is an open access article distributed under the terms and conditions of the Creative Commons Attribution (CC BY) license (<http://creativecommons.org/licenses/by/4.0/>).

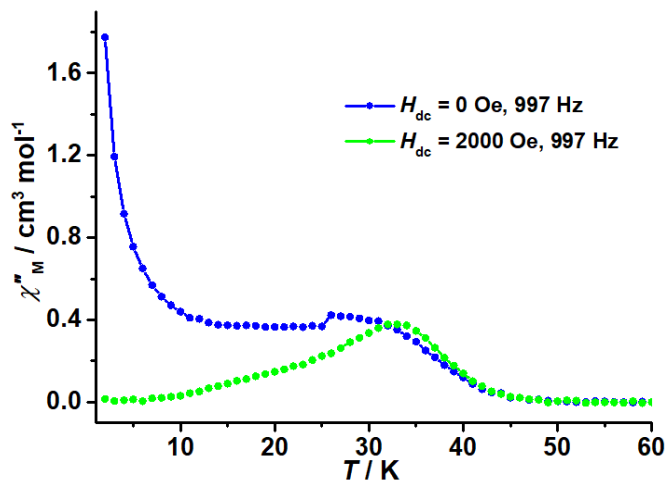


Figure S3. Temperature-dependence of out-of-phase ac susceptibilities (χ''_M) for **1** under 0 Oe and 2000 Oe outer field with frequency of 997 Hz.

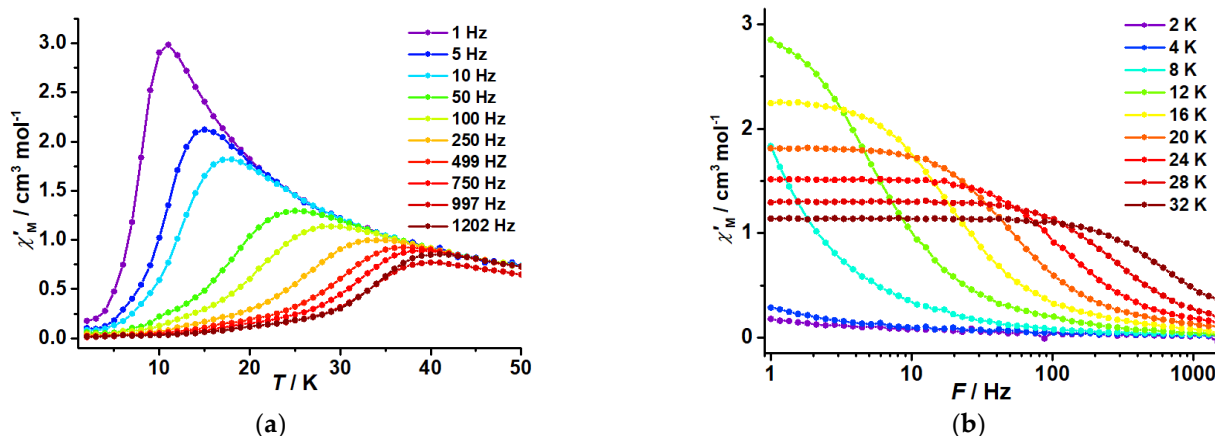


Figure S4. Frequency-dependence of in-phase ac susceptibilities (χ'_M) (a); temperature-dependence of χ'_M (b) for **1** under 2000 Oe field.

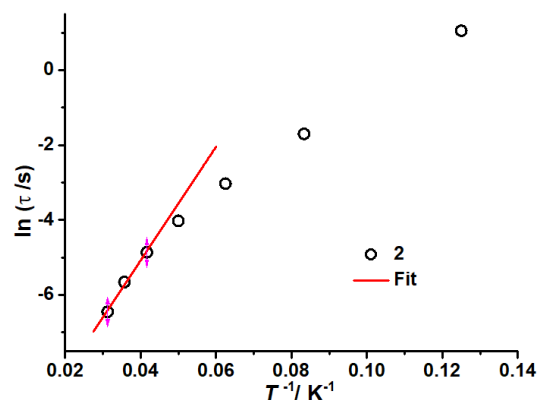


Figure S5. Temperature dependence of magnetic relaxation time τ for **1** under 2000 Oe field. Solid line is the linear fit based on the high temperature data.

3. The Details of *Ab Initio* Calculations

Complete-active-space self-consistent field (CASSCF) calculations on complexes **1** and $[\text{Dy}(\text{L}-\text{c})_2(\text{MeOH})_2]\text{ClO}_4$ [S3] on the basis of single-crystal X-ray determined geometries have been carried out with MOLCAS 8.4 program package [S1].

The basis sets for all atoms are atomic natural orbitals from the MOLCAS ANO-RCC library: ANO-RCC-VTZP for Dy(III) ion; VTZ for close O and N; VDZ for distant atoms.

The calculations employed the second order Douglas-Kroll-Hess Hamiltonian, where scalar relativistic contractions were taken into account in the basis set and the spin-orbit couplings were handled separately in the restricted active space state interaction (RASSI-SO) procedure. For both complexes, active electrons in 7 active orbitals include all *f* electrons (CAS (9 in 7)) in the CASSCF calculation. To exclude all the doubts, we calculated all the roots in the active space. We have mixed the maximum number of spin-free state which was possible with our hardware (all from 21 sextets, 128 from 224 quadruplets, 130 from 490 doublets). SINGLE_ANISO [S2] program was used to obtain the energy levels, *g* tensors, m_J values, magnetic axes, magnetic susceptibilities et al., based on the above CASSCF/RASSI-SO calculations.

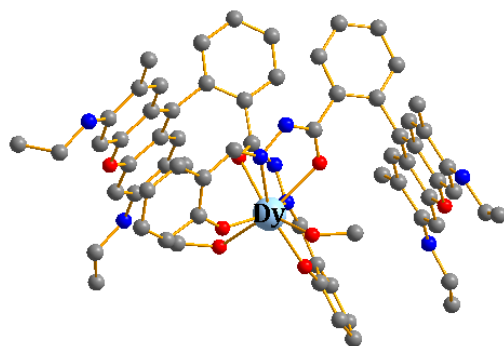


Figure S6. Calculated complete molecular structures of complex **1**. H atoms are omitted.

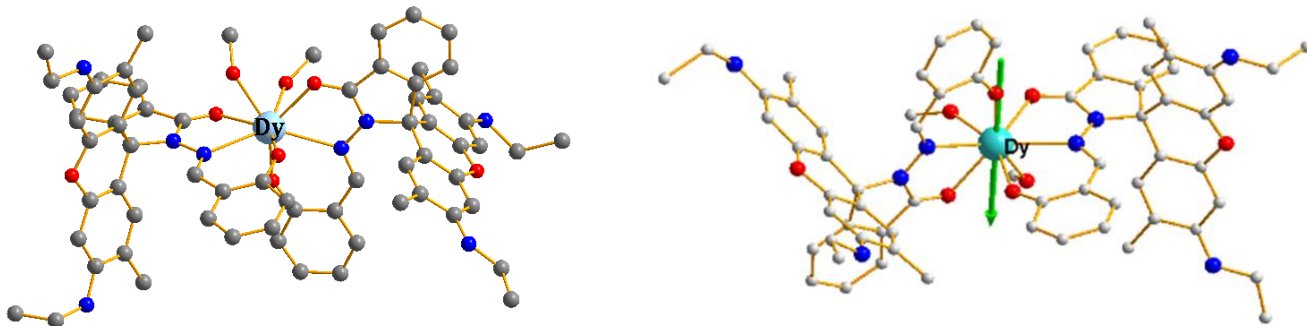


Figure S7. The calculated molecular structures (left) and principal magnetic axes (right) of the ground KDs on Dy(III) of complex $[\text{Dy}(\text{L-}\text{c})_2(\text{MeOH})_2]\text{ClO}_4$ [S3].

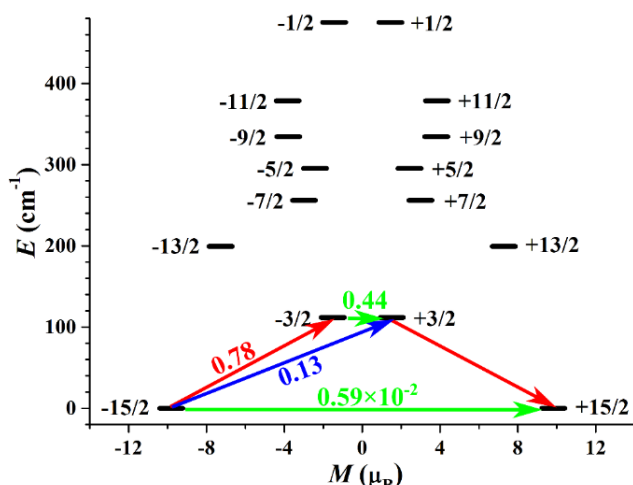


Figure S8. Magnetization blocking barriers in complex $[\text{Dy}(\text{L}-\text{c})_2(\text{MeOH})_2]\text{ClO}_4$ [S3].

4. Coordination Geometry

Table S1. The results of coordination geometric configurations evaluated by SHAPE software for Complex 1.

Lable	Symmetry	Geometric configuration	Deviation parameters
OP-8	D_{8h}	Octagon	31.146
HPY-8	C_{7v}	Heptagonal pyramid	23.902
HPBY-8	D_{6h}	Hexagonal bipyramidal	13.678
CU-8	O_h	Cube	8.407
SAPR-8	D_{4d}	Square antiprism	3.483
TDD-8	D_{2d}	Triangular dodecahedron	1.233
JGBF-8	D_{2d}	Johnson gyrobifastigium J26	14.352
JETBPY-8	D_{3h}	Johnson elongated triangular bipyramidal J1	24.484
JBTPR-8	C_{2v}	Biaugmented trigonal prism J50	2.269
BTPR-8	C_{2v}	Biaugmented trigonal prism	2.068
JSD-8	D_{2d}	Snub diphenoïd J8	2.894
TT-8	T_d	Triakis tetrahedron	8.613
ETBPY-8	D_{3h}	Elongated trigonal bipyramidal	19.969

5. Fitting Results of Cole-Cole Data

Table S2. Fitting parameters obtained from Cole-Cole for **1** in 2000 Oe field.

T (K)	χ^S ($\text{cm}^3 \text{ mol}^{-1}$)	χ^T ($\text{cm}^3 \text{ mol}^{-1}$)	τ (s)	α
8	0.02786	6.53099	2.84804	0.29613
12	0.07284	3.16986	0.18169	0.16706
16	0.09238	2.32107	0.04815	0.12672
20	0.10828	1.83942	0.01786	0.10405
24	0.11743	1.52907	0.00774	0.08914
28	0.12354	1.30932	0.00349	0.07731
32	0.16011	1.14096	0.00158	0.05541

6. Calculated Parameters from *Ab Initio*

Table S3. Calculated energy levels (cm^{-1}), g (g_x, g_y, g_z) tensors and predominant m_J values of the lowest eight Kramers doublets (KDs) for complex **1**.

KDs	1		
	E/cm^{-1}	g_x, g_y, g_z	m_J
1	0.0	0.001, 0.002, 19.711	$\pm 15/2$
2	254.3	0.099, 0.175, 16.080	$\pm 13/2$
3	337.5	0.661, 0.768, 13.350	$\pm 11/2$
4	405.2	0.255, 0.866, 11.921	$\pm 9/2$
5	467.3	3.685, 4.840, 10.493	$\pm 7/2$
6	527.8	2.562, 3.166, 14.292	$\pm 3/2$
7	610.7	0.558, 1.425, 16.827	$\pm 5/2$
8	649.7	0.429, 1.778, 17.378	$\pm 1/2$

Table S4. Wave functions with definite projection of the total moment $| m_J \rangle$ for the lowest two KDs of individual Dy(III) fragments for complex **1** using CASSCF/RASSI with MOLCAS 8.4.

E/cm^{-1}	Wave Functions
0.0	97.6% $ \pm 15/2\rangle$
254.3	80.4% $ \pm 13/2\rangle$ + 13.7% $ \pm 9/2\rangle$

Table S5. Calculated energy levels (cm^{-1}), g (g_x, g_y, g_z) tensors and predominant m_J values of the lowest eight Kramers doublets (KDs) for $[\text{Dy}(\text{L}-\text{c})_2(\text{MeOH})_2]\text{ClO}_4$ [S3].

KDs	$[\text{Dy}(\text{L}-\text{c})_2(\text{MeOH})_2]\text{ClO}_4$		
	E/cm^{-1}	g_x, g_y, g_z	m_J
1	0.0	0.008, 0.027, 19.629	$\pm 15/2$
2	111.8	0.232, 0.350, 18.998	$\pm 3/2$
3	199.4	0.902, 2.560, 14.778	$\pm 13/2$
4	256.2	0.510, 3.783, 13.733	$\pm 7/2$
5	295.4	0.490, 2.353, 13.191	$\pm 5/2$
6	334.5	0.196, 2.363, 8.124	$\pm 9/2$
7	378.5	2.894, 6.451, 12.295	$\pm 11/2$
8	475.2	0.072, 0.232, 18.739	$\pm 1/2$

Table S6. Wave functions with definite projection of the total moment $|m_J\rangle$ for the lowest two KDs of individual Dy(III) fragments for $[\text{Dy}(\text{L}-\text{c})_2(\text{MeOH})_2]\text{ClO}_4$ [S3] using CASSCF/RASSI with MOLCAS 8.4.

E/cm^{-1}	Wave Functions
0.0	98.1% $ \pm 15/2\rangle$
111.8	34.7% $ \pm 1/2\rangle$ + 29.3% $ \pm 3/2\rangle$ + 18.8% $ \pm 5/2\rangle$ + 9.3% $ \pm 7/2\rangle$

References

1. Aquilante, F.; Autschbach, J.; Carlson, R.K.; Chibotaru, L.F.; Delcey, M.G.; De Vico, L.; Galván, I.F.; Ferré, N.; Frutos, L.M.; Gagliardi, L.; et al. Molcas 8: New capabilities for multiconfigurational quantum chemical calculations across the periodic table. *J. Comput. Chem.* **2016**, *37*, 506–541, doi:10.1002/jcc.24221.
2. Chibotaru, L.F.; Ungur, L.; Soncini, A. The Origin of Nonmagnetic Kramers Doublets in the Ground State of Dysprosium Triangles: Evidence for a Toroidal Magnetic Moment. *Angew. Chem. Int. Ed.* **2008**, *47*, 4126–4129, doi:10.1002/anie.200800283.
3. Liu, M.-J.; Fu, Z.-Y.; Sun, R.; Yuan, J.; Liu, C.-M.; Zou, B.; Wang, B.-W.; Kou, H.-Z. Mechanochromic and Single-Molecule Magnetic Properties of a Rhodamine 6G Dy(III) Complex. *ACS Appl. Electron. Mater.* **2021**, *3*, 1368–1374, doi:10.1021/acsaelm.0c01132